Environment and Planning B: Planning and Design 2010, volume 37, pages 942 – 954

doi:10.1068/b36039

Clustering patterns of urban built-up areas with curves of fractal scaling behaviour

Isabelle Thomas
FRS-FNRS, CORE, and Department of Geography, Université catholique de Louvain, Voie du Roman Pays, 34 B-1348, Louvain-la-Neuve, Belgium;
e-mail: isabelle.thomas@uclouvain.be

Pierre Frankhauser
THEMA (CNRS UMR 6049), Université de Franche-Comté, Besançon, France;
e-mail: pierre.frankhauser@univ-fcomte.fr

Benoit Frenay
Machine Learning Group, Université catholique de Louvain, Louvain-la-Neuve, Belgium;
e-mail: Benoit.Frenay@uclouvain.be

Michel Verleysen
Machine Learning Group, Université catholique de Louvain, Louvain-la-Neuve, Belgium; and SAMOS-MATISSE, Université Paris 1 Panthéon-Sorbonne, Paris, France;
e-mail: michel.verleysen@uclouvain.be
Received 23 March 2009; in revised form 19 October 2009; published online 28 June 2010

Abstract. Fractal dimension is an index which can be used to characterize urban areas. The use of the curve of scaling behaviour is less common. However, its shape gives local information about the morphology of the built-up area. This paper suggests a method based on a *k*-medoid for clustering these curves. It is applied to forty-nine wards of European cities, and shows that the curves add interesting intraward information to our knowledge of the spatial variation of the urban texture. Moreover, morphological similarities are observed between cities: living, architectural, and planning trends are not specific to individual cities.

1 Introduction

The analysis of urban built-up areas is a fascinating and complex topic (Batty, 2005; Conzen, 2001; Levy, 1999). Fractals have considerable potential for describing, measuring, analyzing, and modelling complex realities, whatever the field of application (ecology, physics, remote sensing, etc) (eg see Halley et al, 2004). An interesting aspect of fractals for urban geographers is their ability to summarize the complexity, compactness, and heterogeneity of a spatial distribution in a single value (the fractal dimension, denoted D) that is independent of scale (eg see Batty, 2005; Frankhauser, 1998a; 2008; Lam and de Cola, 2002; Lorenz, 2003; Salingaros, 2003).

In this paper we discuss the use of a less common fractal output: the curve of scaling behaviour, which may provide interesting spatial information about the organization of urban patterns at different scales. The curve of scaling behaviour is complementary to the fractal dimension, which is a more global index. When computing curves for several built-up areas, it is interesting to compare their shapes not only visually but also quantatively. In this paper we suggest the use of a *k*-medoid algorithm for this purpose (section 2.3) and apply the method to forty-nine European wards (section 3). The curve of scaling behaviour is seen as an interesting complementary morphometrical measurement, a local index of morphology. Both indicators (fractal dimension and curve of scaling behaviour) should be part of the geographer's toolbox for exploratory spatial data analysis of urban morphologies.

Our results differ from those presented by Thomas et al (2009) where the fractal dimension was 'simply' measured on a larger set of urban wards; it made no reference to curves of scaling behaviour. The two papers are methodologically complementary.

2 Methodological aspects

Binary images are used here: black pixels correspond to built-up areas and white pixels to open spaces. We tested whether the spatial distribution of the black pixels followed a fractal law. A practical example of output is presented in the appendix. The fractal dimension is first explained (section 2.1), and then the curve of scaling behaviour (section 2.2) is considered. Section 2.3 presents a method for clustering places according to the shape of their curve of scaling behaviour.

2.1 Fractal dimension(s)

Fractal dimension is a quantity indicating how completely a fractal fills the space being studied as one zooms down to finer and finer scales. There is no unique way of defining and estimating the fractal dimension (D); here it is computed by means of a correlation analysis (eg see Grassberger and Procaccia, 1983). A small square window of size ε surrounds each built-up pixel. The number of built-up pixels in each window is then counted, which allows the mean number of pair correlations $\mathrm{N}(\varepsilon)$ per window to be computed. This operation is repeated for windows of different sizes. This results in a series of measurements that can be represented on a Cartesian graph, where the X-axis is the size of the window ε, and the Y-coordinate is the mean number of points per window (see the appendix).

The next step consists of fitting this empirical curve to a theoretical curve that corresponds to a fractal law; that is, a power law which links the number of correlations to the size of the window:

$$\mathrm{N}(\varepsilon) = a\varepsilon^{D} , \tag{1}$$

where a is the prefactor of shape, and summarizes the nonfractal morphological properties of the geometric object being analyzed (for a discussion see eg, Frankhauser, 1998b; Gouyet, 1996; Thomas et al, 2009). It can be interpreted as a synthetic indicator of the local particularities of the pattern across scales, due mainly to the fact that the elements of the built-up structure do not have the same shape. For instance, the sizes of the buildings in a residential area (such as detached houses) differ from the sizes of those in an industrial zone. Hence, even if the scaling behaviour and the fractal dimension are the same for both patterns, the mass $\mathrm{N}(\varepsilon)$ differs because the base lengths of the buildings are different. The meaning of a becomes clearer when the identity $a \equiv b^{D}$ is introduced into equation (1):

$$\mathrm{N}(\varepsilon) = a\varepsilon^{D} = b^{D}\varepsilon^{D} = (b\varepsilon)^{D} = (\varepsilon')^{D} = \mathrm{N}(\varepsilon') .$$

In a sense, b corresponds to the average base length of the buildings, which are the constitutive elements of the urban patterns. Differences in b-values also appear when two patterns that have been digitized in different ways are compared; that is, when the sizes of the pixels differ. Hence, in this study the size of the pixel was controlled and fixed at 4 m.

In real-world patterns, fractal behaviour can change across scales. Frankhauser (1998a; 2008) has shown that such changes often occur within rather small ranges of ε, especially for small distances corresponding to the size of small blocks of houses or courtyards. He suggested the introduction of an additional parameter c that allows the estimation of D and a by acting on the overall position of the power-law curve. The enlarged fractal then becomes:

$$\mathrm{N}(\varepsilon) = a\varepsilon^{D} + c . \tag{2}$$

A nonlinear regression is here used for estimating *a*, *D*, and *c* that best fit the empirical curve (appendix).

The fractal dimension of a built-up area can take any value between 0 and 2. When $D = 2$ the built-up pattern is uniformly distributed. $D = 0$ corresponds to a limiting case in which the pattern is made up to one single point (eg a single farm building surrounded by fields). $D < 1$ corresponds to a pattern of disconnected elements (a number of built-up clusters separated one from another). $D > 1$ indicates connected elements [1] forming large and small clusters, in which isolated elements may also occur. The closer *D* is to 2, the more the elements are connected to each other and belong to one single large cluster. From experience, we know that *D* provides quite a good indicator of the morphology of a built-up area (eg see Batty, 2005; De Keersmaecker et al, 2003). The absolute value of *D* is slightly influenced by the estimation technique, the size of the window, and the centring of the window, but these factors do not affect the relative variations and operational conclusions (eg see Thomas et al, 2007).

2.2 Curve of scaling behaviour

In this section we introduce an alternative representation of the empirical results of a fractal analysis: the 'curve of scaling behaviour' (Frankhauser, 1998a). Palmer (1988) called this a 'fractogram', but this terminology is limited to ecology (Leduc et al, 1994). In urban analysis the curve of scaling behaviour has been used up to now only for defining critical scales where the fractal behaviour changes; it has often been used to redefine the size of the window (see Frankhauser, 1989a; 1998b; 2004; Tannier and Pumain, 2005). Batty (2001) used this type of representation, which he called 'signature', to analyze simulated urban patterns.

In this paper we consider the potential use of the curve of scaling behaviour for further characterizing the morphology of urban areas. Let us recall the underlying logic of this type of representation. For this purpose, we start with the original fractal law in equation (1). Taking the logarithm [2] of this relation yields

$$\log \mathrm{N}(\varepsilon) = \log a + D \log \varepsilon \ ,$$

which corresponds to a linear relationship between $\log \mathrm{N}(\varepsilon)$ and $\log \varepsilon$. Hence, we obtain

$$\frac{\mathrm{d} \log \mathrm{N}(\varepsilon)}{\mathrm{d} \log \varepsilon} = D \ ,$$

where *D* corresponds to the constant slope value in the linear relation. However, as already pointed out, the fractal dimension may depend on the scales of the real-world patterns. Then *D* becomes a function of the scale ε [that is, $D = \mathrm{D}(\varepsilon)$]. It is also possible that the typical shape of the objects depends on the scale. In this case this would mean that the shapes of house blocks or town sections are not the same as those of buildings, which implies that the prefactor *a* is a function of ε.

If we assume that the prefactor *a* and the fractal dimension *D* both depend on the distance parameter, we obtain:

$$\log \mathrm{N}(\varepsilon) = \log a(\varepsilon) + \mathrm{D}(\varepsilon) \log \varepsilon \ ,$$

and thus the variation of $\log \mathrm{N}(\varepsilon)$ with respect to $\log \varepsilon$ becomes (Frankhauser, 1998a):

$$\frac{\mathrm{d} \log \mathrm{N}(\varepsilon)}{\mathrm{d} \log \varepsilon} \equiv \alpha(\varepsilon) = \frac{\mathrm{d} \log a(\varepsilon)}{\mathrm{d} \log \varepsilon} + \frac{\mathrm{d} \mathrm{D}(\varepsilon)}{\mathrm{d} \log \varepsilon} \log \varepsilon + \mathrm{D}(\varepsilon) \ . \qquad (3)$$

[1] In this paper, connectivity is always considered from a fractal point of view.
[2] The symbol log has been used since the base of the logarithm does not matter in the given context.

According to equation (3), $\alpha(\varepsilon)$ is equal to a constant D-value, if neither a nor D depend on ε. However, two additional terms contribute to $\alpha(\varepsilon)$: one refers to variations in the shape of the elements which do not affect the fractal behaviour (that is, the hierarchical organization of the pattern) and the other describes the changes of fractal behaviour across scale.(3) Due to these terms, the α-values may exceed the upper limit value of $D = 2$.

Parameter $\alpha(\varepsilon)$ describes the relative changes in the built-up mass $\mathrm{N}(\varepsilon)$ with respect to the relative change in the distance. Indeed given that

$$\mathrm{d}\log \mathrm{N}(\varepsilon) = \frac{\mathrm{dN}(\varepsilon)}{\mathrm{N}(\varepsilon)}; \qquad \mathrm{d}\log\varepsilon = \frac{\mathrm{d}\varepsilon}{\varepsilon},$$

we obtain

$$\alpha(\varepsilon) \equiv \frac{\mathrm{d}\log \mathrm{N}(\varepsilon)}{\mathrm{d}\log\varepsilon} = \left(\frac{\mathrm{dN}(\varepsilon)}{\mathrm{N}(\varepsilon)}\right)\Big/\left(\frac{\mathrm{d}\varepsilon}{\varepsilon}\right).$$

This is a generalization of the usual allometric relationship that is typical of fractals.

Empirical curves of scaling behaviour $\alpha(\varepsilon)$ do—of course—not allow distinguishing between the two types of contributions to equation (3); that is, the variation of $\alpha(\varepsilon)$ and that of $\mathrm{D}(\varepsilon)$. We may, however expect they provide detailed information to what extent the spatial organization of an urban pattern changes across scales or remains constant. Experience shows that the variation of $\alpha(\varepsilon)$ and $\mathrm{D}(\varepsilon)$ usually do not affect the quality of the fit between the empirical curve and the estimated curve (2). Indeed, when measuring the quality of adjustment between the empirical curve and the estimated curve by an R^2 coefficient, we consider the fit between the two curves as 'poor' when $R^2 < 0.9999$; in these cases, we can either conclude that the studied pattern is not fractal, or that it is multifractal (see Tannier and Pumain, 2005). Hence fractal dimension plays the role of a still-valid mean indicator for scaling behaviour.

2.3 Clustering curves

The shape of the curve of scaling behaviour $\alpha(\varepsilon)$ reveals intraward spatial structures. By visually comparing the curves, we can distinguish different types of shapes, but it is not obvious either how to find objective criteria for defining homogeneous groups of curves, nor how to set the number of groups. This question is a rather standard question in data analysis, and is known under the name *clustering*. Clustering consists of grouping data together according to some appropriate criterion; in our case the objects are the curves of scaling behaviour, and the criterion is shape similarity.

Methods traditionally used by geographers are here not applicable: linear correlation does not assess the resemblance between two shapes. The relationship between two shapes can be nonlinear (horizontal or vertical shifts, rotations, etc), whereas correlation measures only linear relationships. Other methods better known in statistics and data analysis overcome this limitation. Among them, the most widely known and used is probably the k-means algorithm. The k-means algorithm consists in (i) finding groups (called clusters) of objects (here: curves) that are similar (here: in shapes), and (ii) for each group finding a representative, which is usually simply the mean—or centre of gravity or centroid—of the objects.

However, the k-means suffers from a drawback which concerns the interpretability of the results: the centroid of experimental data is often not one of the experimental data.

(3) Remember that we assume here that c is a global parameter which does not vary with scale. It may be interpreted as a general error term which summarizes other random errors. Then we may rewrite the relationship $\mathrm{N}(\varepsilon) = a\varepsilon^D + c$ simply as $\mathrm{N}(\varepsilon) - c \equiv \mathrm{N}'(\varepsilon) = a\varepsilon^D + c$, which allows us to proceed to the subsequent steps.

Therefore, we here use a slightly different version of k-means which is called k-medoid, where the representative of each cluster is forced to be one of the initial pieces of data forming the cluster. As an example, let us imagine for the simplicity of the representation that the data are two-dimensional objects; that is, points in a two-dimensional space, instead of curves. Figure 1 shows the difference between the centroid and the medoid of the cluster formed by the six illustrated data points: the centroid is the point in the space which is on average closest to each datapoint, while the medoid is the datapoint from the initial set which is on average closest to the other datapoints.

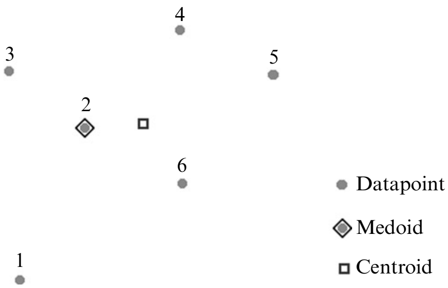

Figure 1. The difference between a centroid and a medoid.

The k-medoid algorithm (Bishop, 2006) works as follows. Given a set of curves $\alpha_1, \ldots, \alpha_n$, the k-medoid algorithm produces a clustering $C = \{C_1, \ldots, C_m\}$ where the m clusters are characterized by the medoids $g_1, \ldots, g_m$. These medoids are chosen from the n curves: C_k contains the curves that are closer to g_k than to any other medoid. More precisely, this algorithm finds the minimum of the function

$$\mathrm{J}(C) = \sum_{k=1}^{m} \mathrm{J}(C_k) = \sum_{k=1}^{m} \sum_{\alpha_i \in C_k} \delta(\alpha_i, g_k)^2 , \tag{4}$$

where $\delta(\alpha_i, g_k)$ is the dissimilarity between the curve α_i and the medoid g_k. Finding the minimum of equation (4) gives a set of m medoids that best represent the set of n curves $\alpha_1, \ldots, \alpha_n$ into m clusters. To find the minimum of equation (4), the k-medoid algorithm proceeds into two steps: it first computes the dissimilarity $\delta(\alpha_i, \alpha_j)$ between each pair of curves α_i and α_j, and then it minimizes $\mathrm{J}(C)$.

Let us first consider the computation of the dissimilarity $\delta(\alpha, \alpha')$ between the two curves $\alpha = (\alpha^1, \ldots, \alpha^T)$ and $\alpha' = (\alpha'^1, \ldots, \alpha'^T)$ where α' is the ith point of α. A simple solution (see figure 2) is to define

$$\delta(\alpha, \alpha') = \sum_{i=1}^{T} (\alpha^i - \alpha''^i)^2 , \tag{5}$$

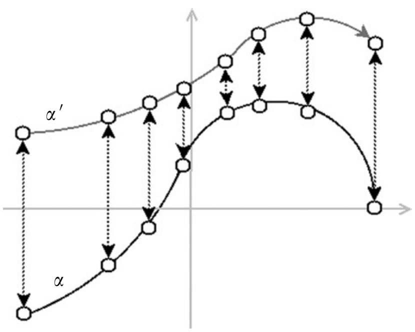

Figure 2. Naive matching between two α-curves.

that corresponds to the Euclidean distance between the two curves α and α'. However, in this case both curves should contain the same number of points, which is not necessarily the case. Moreover, remember that we are interested in a *shape* similarity between curves; this implies that horizontal and vertical shifts between curves should be taken into account. Figure 2 illustrates the Euclidean distance by curves α and α'; obviously, horizontal shifts are not taken into account.

A better solution (figure 3) is to (i) find a suitable matching between the point of α and α', and (ii) then to compute the distance between the matched points. In other words, we do not necessarily compare the ith feature of α with the ith feature of α': the matching given the jth feature of α' which seems to correspond to the ith feature of α and then we compare them. In practice, this match is computed using dynamic programming.

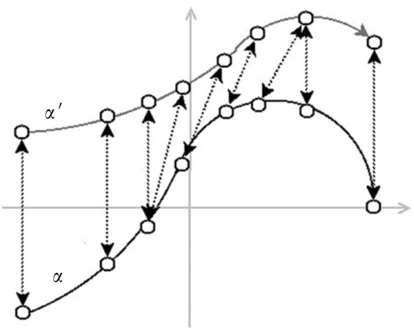

Figure 3. Optimal matching between two α-curves.

Once the distances between all pairs of curves have been computed, the k-medoid algorithm can find the minimum of equation (4). It starts with a random clustering and proceeds in two steps. Firstly, it finds the medoid g_i of each cluster C_i, that is, the curve in C_i which is closest to the other curves in C_i. Secondly, each curve α_i is assigned to the cluster C_j whose medoid g_j is closest to α_i. These two steps are repeated iteratively: the medoids are again updated, then the curves are assigned to their clusters, and so on as long as $\mathrm{J}(C)$ continues to decrease. As it can be shown that $\mathrm{J}(C)$ never increases, the iterative process necessarily stops, in practice after a few iterations only. Note that there is no guarantee that the global minimum of equation (4) is reached; most often, a local minimum is obtained. The easiest way to get an efficient solution is then to repeat the whole process with different initial conditions, and to choose the result that gives the lowest $\mathrm{J}(C)$ criterion.

3 Clustering European urban wards: empirical results

In this section we cluster curves of scaling behaviour computed on European urban wards using the k-medoid method.

3.1 Data

The morphology of the built-up elements of forty-nine town sections form the dataset for this analysis. These wards come from nine European cities: Besançon, Cergy-Pontoise, Lille, Lyon, and Montbéliard in France, Brussels and Charleroi in Belgium, and Stuttgart and the Ruhr area in Germany. A resolution of 4 m per pixel was adopted for all wards. There were two main guidelines for selecting the wards: similar functional areas and very specific built-up textures [for more information see Thomas et al (2009)].

We limit ourselves to considering built-up areas, without knowing the exact function of the buildings (residential, service, industrial, etc). The open spaces (white pixels) are considered as lacunae or 'green areas' (see section 1). We know that there is a bias here that we could not avoid: these open areas or empty cells include roads. In order to minimize this bias, we avoided choosing wards containing large transportation infrastructures, such as railway stations or major roads.

A window was specified around each urban section in such a way that it included the built-up area that had been visually selected; the fractal dimension was computed on this window. Very small windows were avoided, following the principle that the error increases as the number of observations falls; the ratio between the size of the object and that of the window is always smaller than 1, in order to avoid measuring artefacts.

A measuring protocol was defined and applied. This ensured rigorous control of the quality of the estimate and avoided measurement artefacts (De Keersmaecker et al, 2003; Thomas et al, 2009). The same method, with the same control parameters and the same threshold values, was used for all the windows.

3.2 Fractal analysis

The fractal dimension in this dataset ($n = 49$) has an average value of 1.84 and most of the observed values are higher than 1.75 (figure 4). High D-values indicate that the built-up area is homogeneous at different scales, while small D-values reveal heterogeneity: that is, variety in the built-up areas across scales. In our sample of wards, there is some variation between urban wards. Overall, the wards are globally quite homogeneous: the value of the first quartile is very high ($D = 1.92$), and the value of the median (1.86) is above the mean value. Large values of D are associated with small variations of a (figure 5) and R^2 (not illustrated here). The a-values are here always smaller than 2, confirming the fractal nature of the phenomenon. As expected, R^2 is always higher than 0.9999 and increases with D: the higher the value of D, the denser and more homogeneous the built-up area (that is, the larger its mass), and, hence, the more urbanized it is (see also Frankhauser, 2008; Thomas et al, 2007). These first results correspond to our expectations: the history and geography of the city matter, and no clear-cut country effect is visible (see Thomas et al, 2009).

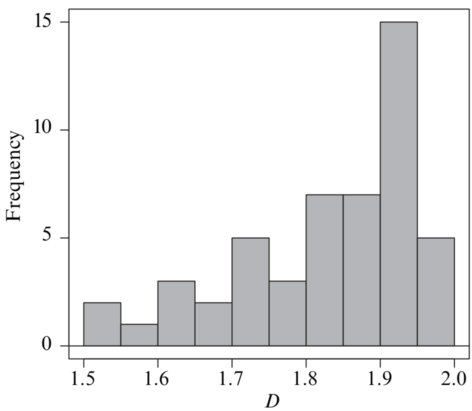

Mean: 1.835
Standard deviation: 0.113

Figure 4. Statistical distribution of D.

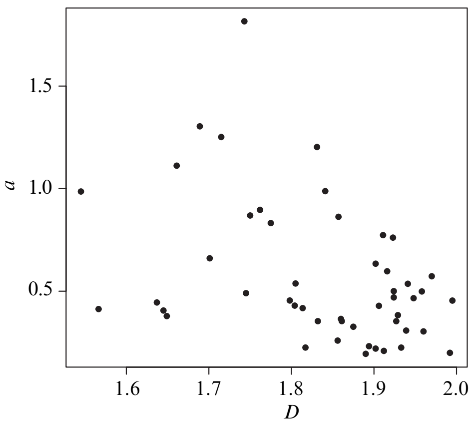

Figure 5. Relationship between fractal dimension (D) and prefactor (a).

As figure 5 suggests, even if D reveals the homogeneity/heterogeneity of built-up space, by itself it is not sufficient to discriminate univocally between two spatial organizations. Different patterns can lead to the same value of D, and a given value of D may correspond to different spatial patterns [for a demonstration see Thomas et al (2007)]. Hence D can only be considered as kind of general index.

3.3 Clustering curves

In spatial analysis it is interesting not only to characterize the morphology of each pattern by one or several indices (section 3.2), but also to see whether some places look alike and why (historical or geographical circumstances). For instance, we expect settlements which grew up during early periods of industrialization to have different patterns from medieval centres or 20th-century new towns. Recent observations seem to confirm such hypotheses (eg see Frankhauser, 2004; 2008; Salingaros, 2003; Thomas et al, 2007; 2008a; 2008b). The aim here is to cluster wards on the basis of the shape of their curve of scaling behaviour. In other words, a curve such as that illustrated in figure A3 in the appendix should be clustered with all other curves having the 'same' shape: that is to say curves with a minimum value at low distances, even if this minimum is placed slightly further farther left or right. This last condition makes the problem trickier than simply the computation of a correlation distance. It was tackled using the k-medoid method described in section 2.3.

Figure 6 shows the value of $\mathrm{J}(C)$ for different numbers of clusters (k). $\mathrm{J}(C)$ decreases as k increases, so that there is no formal criterion for choosing k. For this paper we chose $k = 5$, as a compromise between model error and model complexity. The left column in figure 7 gives the composition of the clusters in terms of curves, while the right column gives one example for each cluster (either the medoid or the area that was visually the most typical).

Let us now compare the clusters in terms of $\mathrm{J}(C)$. For better comparison, we will use the square root of the value divided by the number of curves in the cluster, and label this $\mathrm{AdjJ}(C)$. $\mathrm{AdjJ}(C)$ indicates the average dissimilarity between an α-curve and the medoid of the cluster to which it has been assigned (table 1). The highest values of $\mathrm{AdjJ}(C)$ are observed for clusters 2 and 3. This means that the curves in these clusters are the most diverse (see also figure 7), while clusters 0, 1, and 4 consist

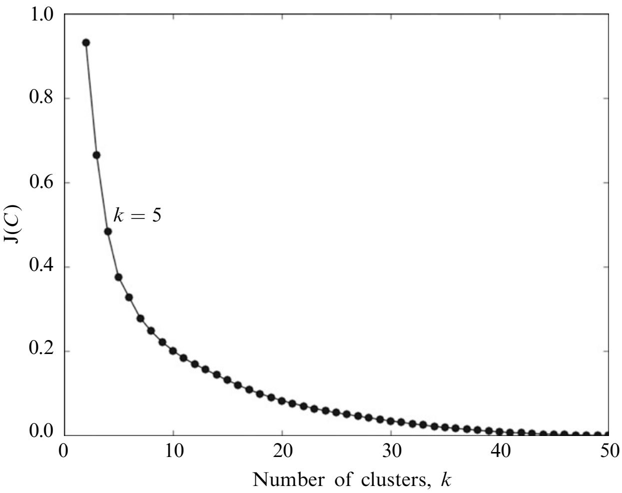

Figure 6. The relationship between $\mathrm{J}(C)$ and the number of clusters, k.

Table 1. AdjJ(C) for the five clusters.

Cluster	AdjJ(C)
0	0.0878
1	0.0668
2	0.1136
3	0.1026
4	0.0773

of curves that look more alike. Surprisingly, these last three groups also have high D-values (figure 8).

Clusters 0 and 4 have the highest average D values ($D > 1.7$) (figure 8); they correspond to more or less 'classic' densely urbanized areas. They often correspond to city centres with root-like built-up patterns (see section 2.2). However, the shape of the scaling curves is different in clusters 0 and 4 (see the left column of figure 7), due to differences in the structure of the built-up areas (right column of figure 7). The analysis of the curves of scaling behaviour has thus provided detailed information about the spatial organization of the urban fabric, since the variation in the fractal behaviour across scales is taken into account.

By looking in more detail at the features of the wards, we can see that cluster 0 corresponds to detached houses aligned along roads (regular organization). The distances between the buildings are small, but white pixels (open spaces) between the buildings are quite numerous. This explains the substantial drop in the scaling behaviour at short distances (figure 7, left). As pointed out above, parameter α links the relative variation in the built-up areas to that of distance, and in cluster 0 the relative variation is low at short distances. This type of fabric often characterizes the suburbs of cities. Cluster 4 has similar D-values to cluster 0 (see figure 8), but a visually different built-up morphology: the curves are much flatter (less variation) and the buildings are more densely packed. They are often terraced. Cluster 4 mostly consists of dwellings in old city centres, mixed with some larger buildings used as offices, schools, shops, etc.

Cluster 2 is heterogeneous in terms of the scaling curves (table 1). There are only three urban wards in this cluster, and they have atypical scaling curves (figure 7). All three come from the new town of Cergy-Pontoise in France, which was created in 1969 to manage the development of the Paris Region in terms of habitat, activities, transport, etc. Cergy-Pontoise has avoided both the role of industrial centre and that of dormitory town, and has succeeded in maintaining the balance between places of work, culture, and habitation. This has led to a certain diversity in its built-up areas, as illustrated in figure 7, with a mixture of large apartment blocks (*barres*) and small detached houses (*pavillonnaires*).

Cluster 3 corresponds to 'pure' Corbusian built-up areas. It consists of social housing (apartment blocks), in quite uniform and regular formations. In France these are called *Les Grands Ensembles*.

Last but not least, cluster 1 consists of areas with buildings covering large irregular areas. These are mainly free-standing industrial or office buildings, where intrabuilding distances are considerable. As illustrated by the curves in figure 7, the scaling behaviour is large at small distances due to the size of the buildings.

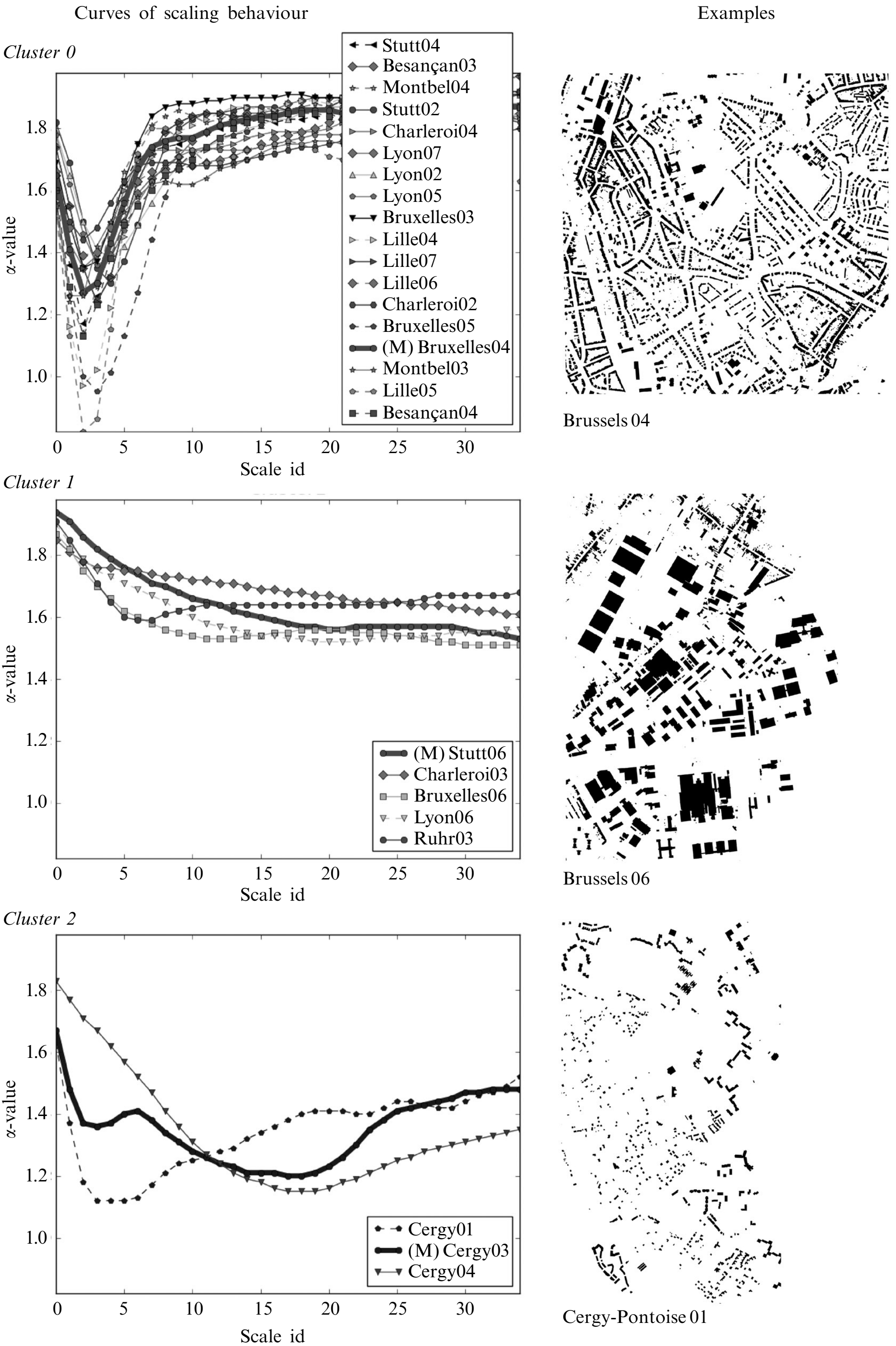

Figure 7. Cluster composition when $k = 5$: curves and one example of each type of urban structure.

Cluster 3

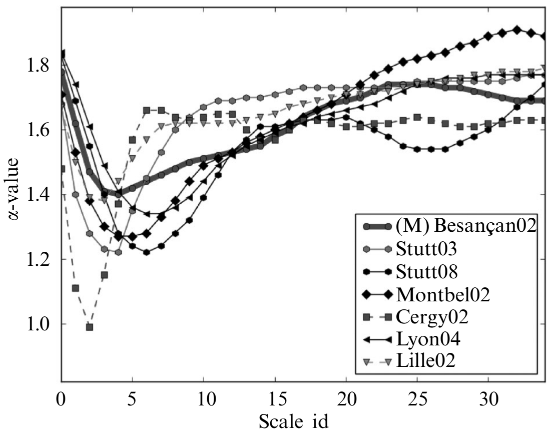

Besançon 02

Cluster 4

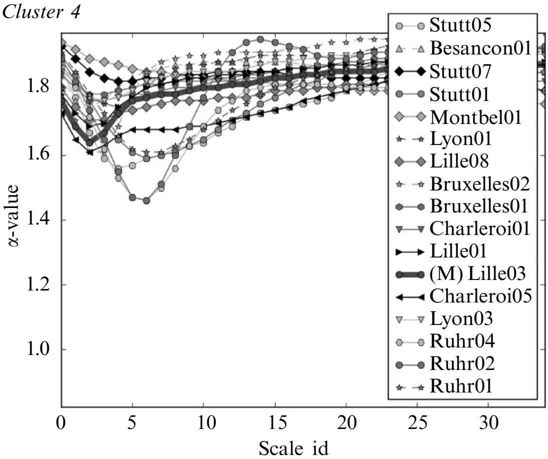

Lille 03

Figure 7 (continued).

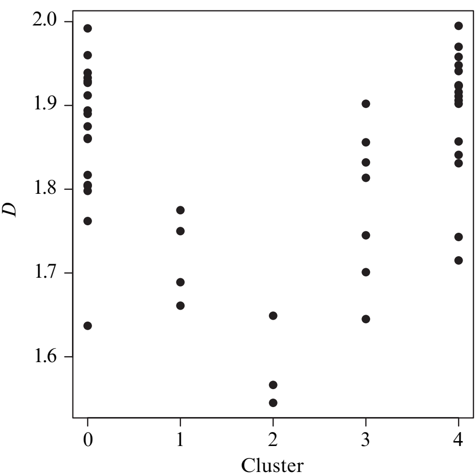

Figure 8. The distribution of the fractal dimensions, *D*, in each cluster.

4 Conclusion

This paper has considered scaling behaviour curves, an output of fractal analysis. These curves illustrate how the two fractal parameters vary across scales. Distance ranges can be identified at which substantial changes in spatial organization occur, or alternatively, for which the parameters are stable. Hence the information contained in these curves turns out to be complementary to that of the fractal dimension D which remains a useful, but rather general, indicator.

An important contribution of this paper is the use of the k-medoid method to cluster the curves of similar shapes. This method is quite similar to that of k-means, but can use dissimilarity measures which are not distances. Here, it allows a dissimilarity to be computed from a matching, which is well suited to curves with horizontal or vertical shifts. It is useful not only for curves of fractal scaling behaviour but also for clustering any other curves in geography (remote sensing, etc). The application to a set of European urban wards showed that the clustering results fit well with planning history (areas with similar histories cluster together). Clustering the curves instead of using only the fractal dimension undoubtedly adds accuracy to the final result in terms of morphometry.

References

Batty M, 2001, ‘Generating urban forms from diffusive growth” *Environment and Planning A* **23** 511 – 544

Batty M, 2005 *Cities and Complexity: Understanding Cities with Cellular Automata, Agent-based Models, and Fractals* (MIT Press, Cambridge, MA)

Bishop C, 2006 *Pattern Recognition and Machine Learning* (Springer, Berlin)

Conzen M, 2001, “The study of urban form in the United States” *Urban Morphology* **5**(1) 3 – 14

De Keersmaecker M L, Frankhauser P, Thomas I, 2003, “Using fractal dimensions to characterize intra-urban diversity: the example of Brussels” *Geographical Analysis* **35** 310 – 328

Frankhauser P, 1998a, “The fractal approach: a new tool for the spatial analysis of urban agglomerations” *Population* **4** 205 – 240

Frankhauser P, 1998b, “Fractals geometry of urban patterns and their morphogenesis” *Discrete Dynamics in Nature and Society* **2** 127 – 145

Frankhauser P, 2004, “Comparing the morphology of urban patterns in Europe—a fractal approach”, in *European Cities: Insights on Outskirts* Eds A Borsdorf, P Zembri (ESF COST Office, Brussels) pp 79 – 105

Frankhauser P, 2008, “Fractal geometry for measuring and modelling urban patterns”, in *The Dynamics of Complex Urban Systems: An Interdisciplinary Approach* Eds S Albeverio, D Andrey, P Giordano, A Vancheri (Physica, Heidelberg) pp 213 – 243

Gouyet J F, 1996 *Physique et Structures Fractales* 2nd edition (Masson, Paris)

Grassberger P, Procaccia I, 1983, “Measuring the strangeness of a strange attractor” *Physica D* **9** 189 – 208

Halley J, Hartley S, Kallimanis A, Kunin W, Lennon J, Sgardelis S, 2004, “Uses and abuses of fractal methodology in ecology” *Ecology Letters* **7** 254 – 271

Lam N, de Cola L, 2002 *Fractals in Geography* (The Blackburn Press, Caldwell, NJ)

Leduc A, Prairie Y, Bergeron Y, 1994, “Fractal dimension estimates of a fragmented landscape: sources of variability” *Landscape Ecology* **9** 279 – 286

Levy A, 1999, “Urban morphology and the problem of the modern urban fabric: some questions of research” *Urban Morphology* **32**(2) 79 – 85

Lorenz W, 2003, “Fractals and fractal architecture”, Vienna University of Technology, http://www.iemar.tuwien.ac.at/fractal_architecture/subpages/01Introduction.html

Palmer M, 1988, ‘Fractal geometry: a tool for describing spatial patterns of plant communities” *Vegetatio* **75** 91 – 102

Salingaros N, 2003, “Connecting the fractal city”, keynote speech, Biennial of Towns and Town Planners in Europe, Barcelona, http://www.zeta.math.utsa.edu/~yxk833/connecting.html

Tannier C, Pumain D, 2005, “Fractales et géographie urbaine: aperçu théorique et application pratique” *Cybergeo* paper 307

Thomas I, Frankhauser P, De Keersmaecker M L, 2007, “Fractal dimension versus density of the built-up surfaces in the periphery of Brussels” *Papers in Regional Science* **86** 287 – 307

Thomas I, Frankhauser P, Biernacki C, 2008a, "The morphology of built-up landscapes in Wallonia, Belgium: a classification using fractal indices" *Landscape and Urban Planning* **84** 99 – 115
Thomas I, Tannier C, Frankhauser P, 2008b, "Is there a link between fractal dimension and residential choice at a regional level?" *Cybergeo* paper 413
Thomas I, Frankhauser P, Badariotti D, 2009, "Comparing the fractality of European neighbourhoods: do national contexts matter?", paper presented at the ERSA 2009 conference in Lödz and at the ASRDLF 2009 in Clermont Ferrand; copy available from the authors

Appendix

Example of a fractal analysis using *Fractalyse* (http://www.fractalyse.org/) on a real-world urban area in Brussels (named Bruxelles04), Belgium.

Figure A1. The studied area.

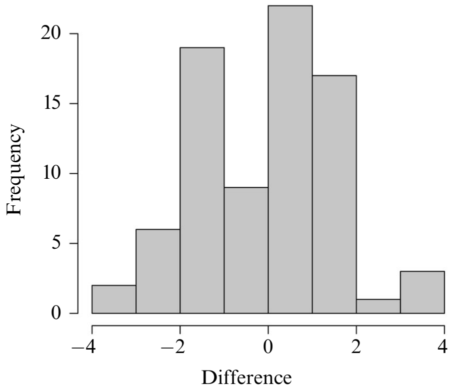

Figure A3. Difference between observed and estimated values of *D*.

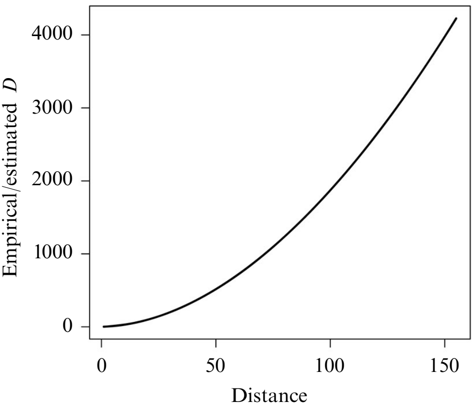

Figure A2. Empirical and estimated *D*-values (2 curves superimposed) according to distance.

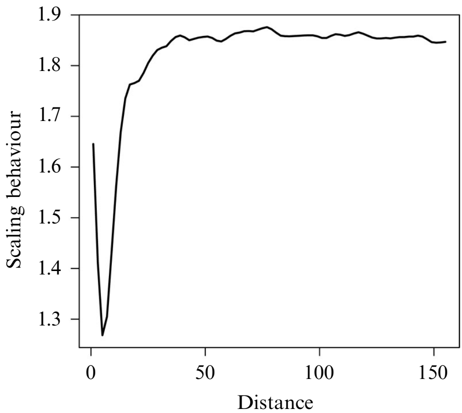

Figure A4. Curve of scaling behaviour.